Archaeological Investigation and Visualization by Ground-Penetrating Radar at Wiang Kaew Palace Site in Chiang Mai City Moat, Thailand

Sriwong Boonprakom* and Suwimon Udphuay
Department of Geological Sciences, Faculty of Science, Chiang Mai University, Chiang Mai, 50200, Thailand.
*Author for correspondence; e-mail address: sriwong_b@cmu.ac.th

ABSTRACT

This study employs ground-penetrating radar (GPR) to investigate the walls of Wiang Kaew palace within the urban environment of the Chiang Mai city moat in Thailand. An 1893 McCarthy map accurately illustrates the existence and location of this ancient palace. In 2018, archaeologists uncovered buried segments of the Wiang Kaew Palace walls. To further explore these buried remains, the 500 MHz radar PulseEkko® system was utilized in accessible prospective areas. The GPR surveys were executed using a grid system, and standard data processing steps were applied to the radar data, accounting for disturbances caused by rebar, wet soil zones, and drainage systems. Diffraction and planar reflection signatures were employed for interpreting the wall structure. The envelope attribute analysis was particularly beneficial in enhancing the migrated data sections. Envelope data were used to generate amplitude depth slices and isosurfaces, aiding in the interpretation and visualization of the wall structure alongside the GPR sections. The GPR data showcases sections of Wiang Kaew palace walls, revealing the surviving portions of the south, front, and north walls. The visualization of Wiang Kaew Palace walls from this study has potential applications in Chiang Mai's urban planning as well as in the realms of archaeological preservation and excavation.

Keywords: ground-penetrating radar, GPR, archaeological investigation, envelope, isosurface

1. INTRODUCTION

Wiang Kaew palace (WKP) was established in the Chiang Mai city moat, as a place for central rulers of Chiang Mai city during Lanna age. 'Wiang Kaew' means all regions of the palace, including its enclosing walls. A historic photograph (Fig. 1a) well illustrates that WKP has walls.

In 1893, the Ministry of Interior prepared 'McCarthy map' of Chiang Mai city [1], shown in Fig. 1b. The map well proves the existence of WKP by the grey-shaded region in Fig. 1c. The palace can be inherently divided into three parts – the front palace, the north rear palace, and the south rear palace enclosed by the front wall, north wall, and south wall, respectively. There is a common middle wall where regions of the north and south rear palace bind. The north and south palaces are L-shaped, while the front palace is rectangular. WKP was constructed during the late 13th century and the mid-17th to early 18th centuries [2].

WKP was abandoned in 1767, although some maintenance and refurbishments were performed in 1794. The palace was transferred into the possession of the Siam government in 1903 [3-5]. WKP reflects Lanna's history and sociology, and it influences Chiang Mai urban planning and tourism. Therefore, it is one of the most important archaeological sites in Chiang Mai city.

Recently, the tobacco warehouse (TW), Wiang Kaew Rd (W), and Inta Rd (R) replaced the north rear palace. Meanwhile, a women correctional institute initially had replaced the south rear palace after it was demolished in 2016. It is now generally known as the Chiang Mai Former Woman Correctional Institute (FWCI or C). The front palace has been replaced by a tobacco office (TO), Jao Duang Deun's house (JDH), recruiter's houses (RCH), and Jaban Rd (J). The overall area is known as the 'Khuang Luang Wiang Kaew Project' (KLWKP).

The remaining structures of WKP are the enclosing walls which were made of bricks. They are sustainable to erosion. However, bricks can be vandalized in some periods. They were investigated by ground-penetrating radar (GPR) performed inside the FWCI by Kasetsart University [6], and some parts of them were proved that they are ancient structures relevant to WKP [2]. The structures are two 150-

m-long walls at 0.6-1.0 m depth with 2.0-2.2 m width, one wall junction, and one ancient canal. The south 150-m-long wall has been reburied in subsurface after excavation in 2018, in order to preserve it.

Ref. [7] and [8] also found brick clusters close to Burirat's house (BH), which is probably a part of related WKP construction. However, the N-S south wall at the western edge of the south-rear palace has not yet been found. The north and front walls under the surrounding urban neighborhoods also have not yet been found. Therefore, this study focuses on GPR investigation and visualization for these walls. This study provides GPR anomaly maps, fence diagrams, and isosurfaces of WKP as preliminary investigation results.

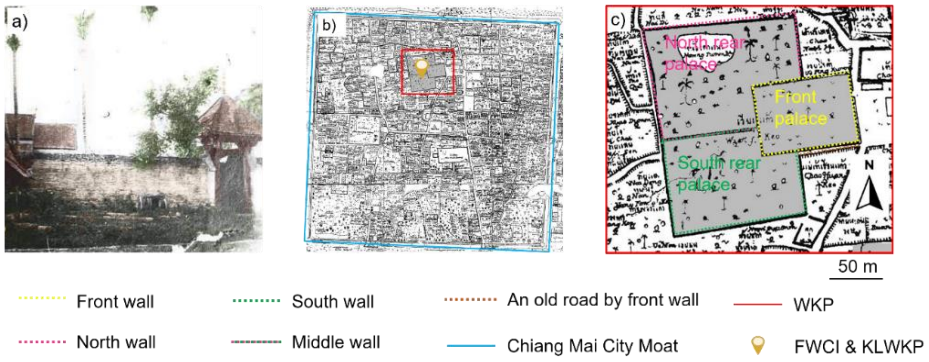

Fig. 1 (a) a wall enclosing the WKP (b) McCarthy map showing Chiang Mai City Moat, WKP, and FWCI and KLWKP highlighted by a blue rectangle, a red rectangle, and a yellow mark, respectively (c) zoomed-in McCarthy map shown the palace with its three parts – northern and southern rear palace and front palace are enclosed by the north wall, south wall, and front wall, respectively. The middle wall divides two rear palaces (modified from [1]).

2. GROUND-PENETETRATING RADAR

In frequency range from 10 MHz to 2 GHz, used in GPR exploration case, electromagnetic (EM) waves travel through earth materials with small electrical conductivity $\sigma < 0.01$ S/m and non-magnetic properties; relative magnetic permeability $\mu_r = 1$. Molecular polarization of water molecules in subsurface medium and interfacial polarization, which are caused by electric field application, play important role in velocity and attenuation of EM wave versus its frequencies [9]. EM propagation through a half-space medium with velocity $v = c/\sqrt{\varepsilon_r}$ when ε_r is a relative dielectric permittivity of subsurface and c is EM waves velocity in vacuum [9-11]. Furthermore, skin depth or penetration depth δ of EM propagation is inverse of attenuation α, expressed as $\delta = 1/\alpha$. In case of GPR, δ depends on electrical conductivity σ, dielectric permittivity ε, and magnetic permeability μ, expressed as $\delta = (2/\sigma)\left(\sqrt{\varepsilon/\mu}\right) = 5.31 \times 10^{-3}\sqrt{\varepsilon_r}/\sigma$. Buried materials cause EM wave reflections conducted in this study. Strength of reflection relies on reflectivity R depending on difference between ε_r of any two layers. It is mathematically expressed by $R = \left(\sqrt{\varepsilon_{r_1}} - \sqrt{\varepsilon_{r_2}}\right)/\left(\sqrt{\varepsilon_{r_1}} + \sqrt{\varepsilon_{r_2}}\right)$ when ε_{r1} is ε_r of the upper layer and ε_{r_2} is ε_r of the lower layer [12-13]. Additionally, the velocity, attenuation, and skin depth of EM waves in GPR exploration are not affected by frequency; the first one is influenced by only the dielectric constant of the subsurface, where the other two are influenced by the electrical conductivity, magnetic permeability, and dielectric constant of the subsurface.

3. SITE DESCRIPTION AND DATA ACQUISITION

WKP site had been settled inside Chiang Mai city moat (Fig. 2a) in Chiang Mai province (Fig. 2b), northern Thailand (Fig. 2c). FWCI and KLWKP (orange pinpoint) are at 498441.85N 2077774.20E zone 47Q UTM geographic referencing. The study area surface is covered by steel-reinforced concrete pavement and sandy-loam soils with vegetation. According to the excavation in 2018, a red-yellow mottled soil at which water accumulates [14] is 50-180 cm depth.

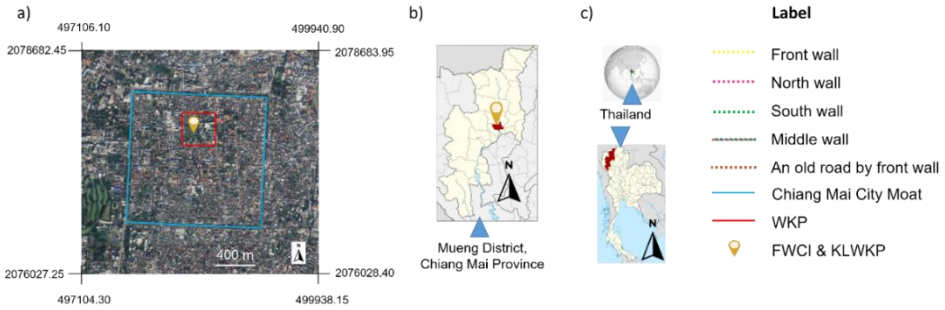

Fig. 2 (a) Satellite view (b) A red region referring to Mueang Chiang Mai district (c) Thailand (green region) and Chiang Mai (red region) shown in Geographical map.

GPR data in this study were collected by the 500 MHz antenna PulseEkko® system (Fig. 3). They were acquired by odometer mode on three types of surfaces. Soil surface with vegetation (Fig. 3a) and concrete surface (Fig. 3b) have EM attenuation from water content/moisture in soil and rebar, respectively. Surface with vegetation soil and concrete (Fig. 3c) has both causes of attenuation for EM propagation.

Fig. 3 GPR data acquisition using 500-MHz PulseEkko® system on (a) vegetation soil surface, (b) concrete surface, and (c) both of surfaces.

There are 40 X-Y GPR grids acquired at accessible sites of WKP (orange-shaded areas in Fig. 4) with 0.25 m line spacing. Numbers of grids acquiring the south wall, front wall, and north wall are 21, 11, and 8, respectively. Near the west end of the south 150-m-long wall, the preserved wall structure inside FWCI was selected to be a GPR test grid shown in Fig 4. The data from this test grid were used to create a ground truth model, enabling a comparison of its results with the entire project's findings and facilitating easier interpretation. A few wide-angle reflection and refraction (WARR) were acquired for the estimation of GPR velocities in the subsurface.

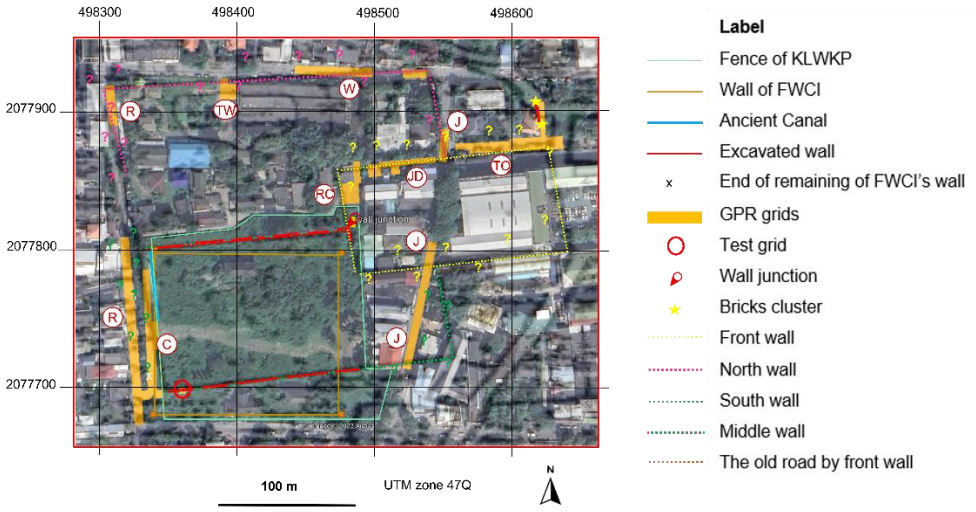

Fig. 4 All assumed walls, excavated wall structure, and GPR grid acquisition area overlain on Google Earth Pro and faint-shading McCarthy map.

4. DATA PROCESSING

Standard processing steps from as follows (step 4.1 to 4.8) are applied to all collected GPR data using Ekko_Project™ software licensed by Sensors & Software Inc. The last step 4.9 is conducted on Voxler version 4 lisenced by Golden Software.

1) Data editing is applied to correct parameters and line direction, sort data, and remove poor quality data.
2) Dewow and DC removal are used to move distorted signal position to its original position or mean zero level and eliminate low-frequency components.
3) Background average subtraction and horizontal filtering are applied for enhancing the signal and removing disturbing diffraction signals from rebars.
4) Bandpass filtering for removing unwanted frequencies components.
5) SEG2 gain for intensifying amplitude at higher two-way-travel time.
6) Those data are interpreted using Fence's diagram of unmigrated sections.
7) Migration is essentially applied for moving EM energy from diffractions to its incident points, using velocity analysis.
8) Hilbert's transformation is used to generate analytic signal and envelope attribute. Finally, those envelope data are combined into cube and generated depth slices of envelope value to find parts of the WKP walls with reasonable identification [15-16].
9) Isosurface, which is rendered from a percentage of envelope value, is utilized for subsurface body visualization [17-18].

4 INTERPRETATION AND DISCUSSION

5.1 South rear palace

A high-amplitude radar anomaly was detected within the test grid, situated at a depth of 60 to 120 cm beneath the surface. This anomaly spans a width of 2 to 3 m and exhibits a consistent lineation in the west-east direction, corresponding to the excavated south wall in this zone during 2018. Consequently, the radar characteristics observed in the test grid can serve as an initial model for interpreting other grids within this project. Furthermore, the appearance of radar reflectors, their width, and lineation align with the findings of the nearest GPR grid acquired by Kasetsart University in 2013. However, it is worth noting that the top of this anomaly is situated 20 to 30 cm deeper than in the Kasetsart University work.

Grids C, R, and J are lineated in almost N-S direction to cover potential areas that might cover the south wall (Fig. 5a). A 50-to-60-cm depth slice of grid C5 shows clear high-amplitude anomalies oriented in the N-S direction, highlighted by black dotted lines in Fig. 5b. Their length is around 17-18 m (including their extending part in C4 and C6). Their width is around 2-3 m. The anomalies are interpreted as an archaeological structure. Additionally, there are two circular zones of low amplitude highlighted by white and orange arrows and a 4-m-wide gap between the north and south structure highlighted by a black arrow. They might have been a vandalized zone since the WKP age, or they could be a pit that had been made for a purpose. Lines X06, X18, X30, X42, and X54 are chosen to generate a fence diagram. An 80-to-90-cm depth slice of Grid J1 shows a W-E moderate-to-high-amplitude anomaly highlighted by black dotted lines in Fig. 5c. It is interpreted as an archaeological structure relevant to a WKP wall since it is close to overlie the W-E WKP wall. Its length and width are 4 and 1 to 3 m, respectively.

The fence diagram of C5 in Fig. 6a shows planar reflectors referring to stacks of a structure that may be a wall. Hyperbolae (red arrows) in the diagram are probably diffractions from bricks inside the wall. Interestingly, lines X06 and X42 cut through the vandalize zones, which should completely have low anomaly (white and orange arrow) between the west structure (red block) and east structure (orange block), but there is a significant amplitude value of reflectors. Therefore, they might be pits inside the wall body, filled with archeological fragments and soil. Line X18 shows faint amplitude since it cuts the gap. The isosurface in Fig. 6b shows 49 percent threshold of amplitude. It shows two parts of the wall body with its east structure where pits appear. The top surface of the wall, pits, and gap are visualized.

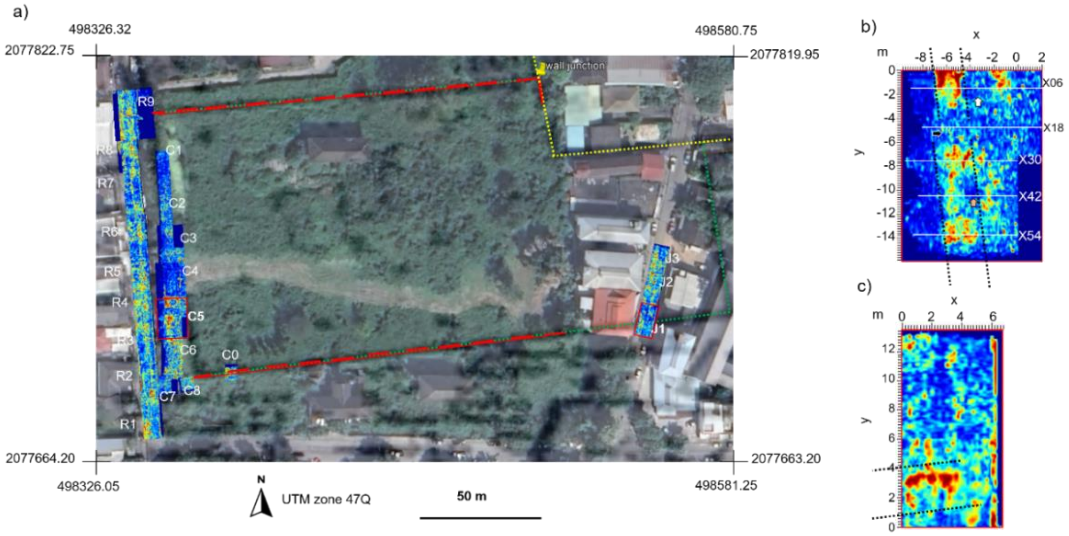

Fig. 5 (a) 60-to-70-cm depth slices from the GPR grid in C, R, and J. C5 and J1 have clear high-amplitude anomalies. (b) A 50-to-60-cm depth slice of Grid C5 with N10^{0}W anomaly lineation highlighted by black dotted lines. White, black, and orange arrows point at vandalize zone. White lines refer to cross sections of the anomaly. (c) A 80-to-90-cm depth slice of Grid J1 with N80^{o}E anomaly lineation highlighted by black dotted line.

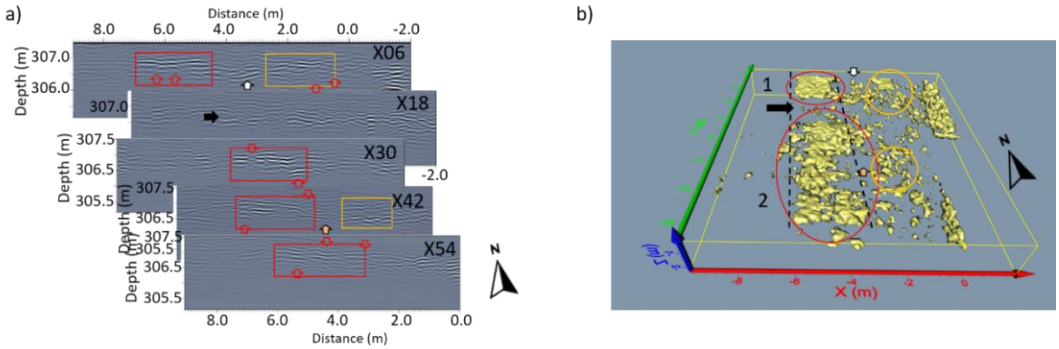

Fig. 6 (a) Fence diagram of selected lines in grid C5 shows strong anomalies in red and orange rectangles. Red arrows label planar reflectors and hyperbolae vertices. White, black, and orange arrows point at weak-amplitude zone. (b) 49-percent isosurface of grid C5 with lineation highlighted by black-dotted lines. Black, orange, and white arrows mark pits and a gap. Ovals are probably archaeological parts of the south wall.

5.2 Front palace

Grids RC, JD, J, and TO cover potential areas that might cover the front wall (Fig. 7a). A 60-to-70-cm depth slice of grid J7 shows apparent high-amplitude anomalies oriented in N80^{o}E and N10^{o}W directions, highlighted by black dotted lines in Fig. 7b. The W-E one is 6 m long and 3-4 m wide. Lines Y03, Y12, and Y21 are chosen for the fence diagram. A 70-to-80-cm depth slice of grid JD3 has a dense N80^{o}E high-amplitude anomaly highlighted by black dotted lines in Fig. 7c. Its length and width are 4 and 1 to 3 m, respectively. The anomalies found in JD3 and J7 are interpreted as archaeological structures relevant to the front wall since they are close to the overlain WKP walls. The fence diagram of J7 in Fig. 8a also shows several planar reflectors referring to a brick stack of the wall. Appearing hyperbolae correspond to well brick-contact condition of the archaeological structure. The isosurface of J7 in Fig. 8b shows 62 percent threshold of amplitude. It shows the surface of a part of the possible wall body lying eastward in a dashed oval.

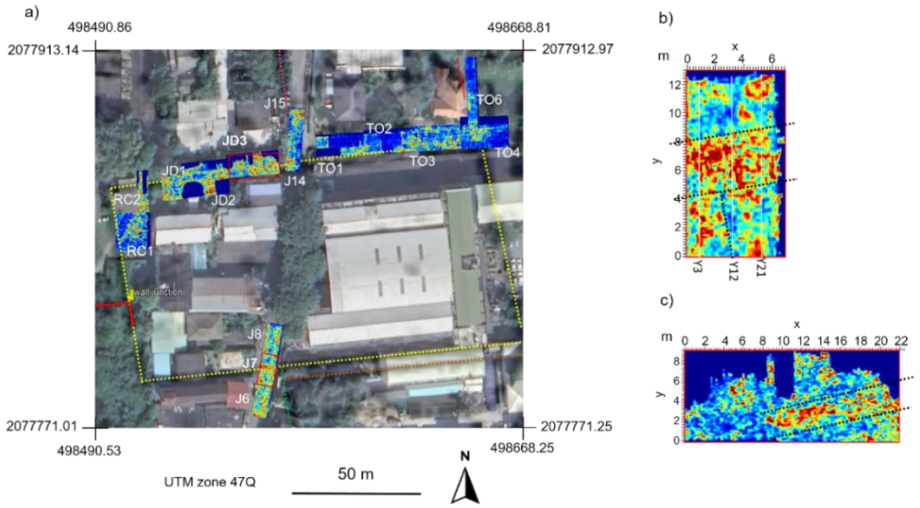

Fig. 7 (a) 80-to-90-cm depth slices from GPR grids in RC, JD, J, and TO. J7 and JD3 have clear high-amplitude anomalies. (b) A 60-to-70-cm depth slice of Grid J7 with N80^{o}E anomaly lineation highlighted by black dotted line. White lines (Y3, Y12, Y21) refer to cross sections of the anomaly. A small N-S anomaly at the southwestern corner of the grid also appears. (c) A 70-to-80-cm depth slice of Grid JD3 with N80^{o}E anomaly lineation highlighted by black dotted line.

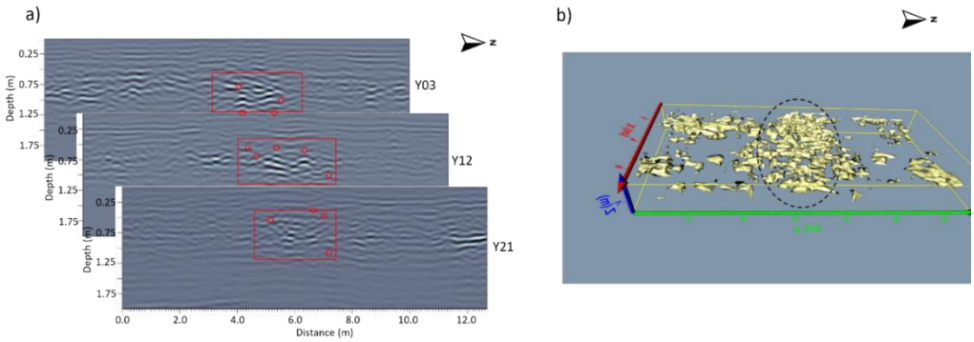

Fig. 8 (a) Fence diagram of selected lines in grid J7 shows strong anomalies in red rectangles. Red arrows label planar reflectors and hyperbolae vertices. (b) 62-percent isosurface of grid J7 with a dashed oval as a probable front wall.

5.3 North rear palace

Grids R, TW, and W cover potential areas that might cover the north wall (Fig. 9a). A 70-to-80-cm depth slice of Grid R11 shows a high-amplitude anomaly number '1' oriented in N10^{0}W direction, highlighted by a black dotted line in Fig. 9b. Its length and width are around 10-12 m (including their extending part in R10) and 2 m, respectively. Anomaly number '2' is a small region at the northeastern corner of the grid. Lines Y24, X04, X10, and X16 are chosen to generate a fence diagram. A 60-to-70-cm depth slice of Grid W5 shows an apparent dense high-amplitude anomaly oriented in the W-E direction, highlighted by black dotted lines in Fig. 9c. Its length and width are 8 to 12 and 1 to 3 m, respectively. The anomalies found in R11 and W5 are interpreted as archaeological structures relevant to the north wall since they are close to the overlain WKP walls. The fence diagram of R11 in Fig. 10a shows wavy reflectors and a few hyperbolae, probably corresponding to good brick-contact conditions but a non-planner-layered wall in both of number '1' and '2'. The isosurface of R11 in Fig. 10b shows 49 percent threshold of amplitude. It shows the surface of two parts of the possible wall body. Number '1' probably is a part of N-S north wall. Number '2' probably is a part of W-E north wall since it is close to the north wall corner.

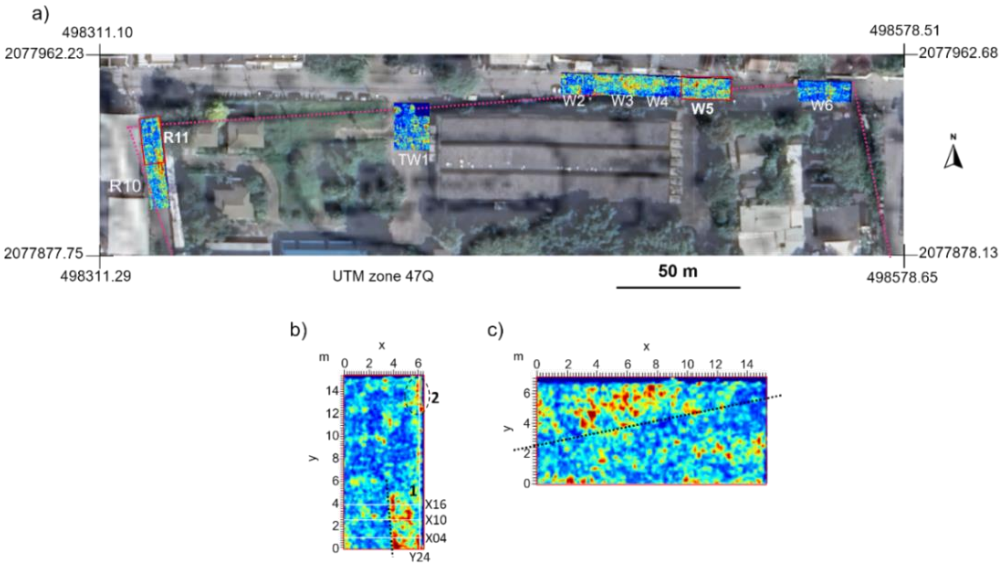

Fig. 9 (a) 70-to-80-cm depth slices from GPR grids in R, TW, and W. Grid R11 and W5 have evident high-amplitude anomalies. (b) A 70-to-80-cm depth slice of Grid R11 with N10^{0}W anomaly number '1' is highlighted by a black dotted line (X04, X10, X16). Anomaly number '2' at the northeast grid is highlighted by an oval. White line (Y24) refers to cross-sections of the anomalies. (c) A 60-to-70-cm depth slice of Grid W5 with N80^{o}E anomaly lineation highlighted by a black dotted line.

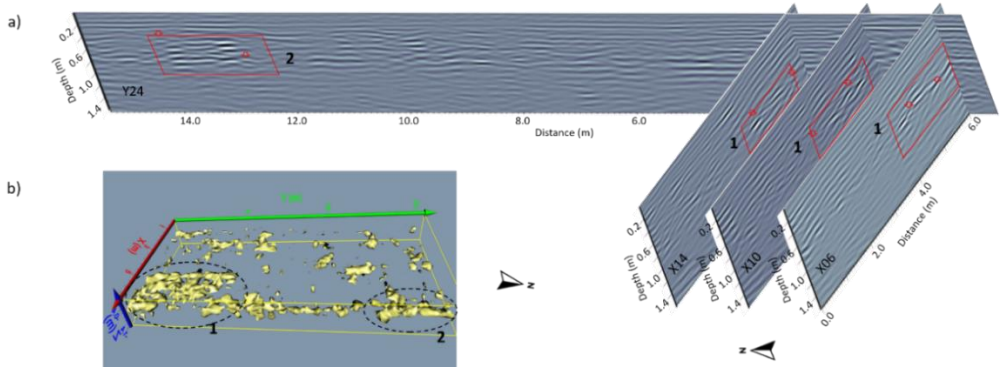

Fig. 10 (a) Fence diagram of selected lines in grid R11 shows strong anomalies in red rectangles number '1' and '2'. Red arrows label planar reflectors and hyperbolae vertices in both numbers. (b) 49-percent isosurface of grid R11 with dashed ovals as a probable north wall.

5 CONCLUSIONS

GPR proves to be a valuable tool for investigation and the identification of potential remains of Wiang Kaew Palace (WKP) walls within the Chiang Mai city moat. Overall results in the south of FWCI partially agree with results from Kasetsart University in terms of amplitude, lineation, the shape of reflectors, and size of anomalies. Nevertheless, the depth of archaeological anomalies in this study is deeper than those reported by Kasetsart University. Depth slices from six grids out of the total forty consistently display lineations of high amplitude anomalies in locations corresponding to the WKP wall's position as indicated on the ancient map. Fence diagrams of unmigrated sections illustrate distinct reflectors and hyperbolae, likely representing arrangements of stacked bricks within the wall structure. Isosurface images provide visualizations of the upper surface of these potential wall structures. To enhance the accuracy of visualizing the wall structure further, we plan to incorporate GPR attribute analysis and new curvelet analysis into our ongoing work.

ACKNOWLEDGEMENTS

I would like to thank Department of Geological Sciences, Faculty of Science, Chiang Mai University for all research facilities. This study has been granted by Thai Development and Promotion of Science and Technology (DPST) scholarship and Annual Research Fund by the Faculty of Science, Chiang Mai University. I also appreciate Saiglang Jindasu, the archaeologist responsible for KLWKP archeology, for providing helpful archaeological data and achieves.

REFERENCES

[1] Meechoobot W., 1893 Nakhon Chiang Mai City Map, Available at: https://www.silpa-mag.com/history/article_43486. (in Thai)

[2] Jindasu S., *Wijai Wijak Academic Conference 2018 by Fine Arts Department*, Chiang Mai, Thailand, 24 Sep – 25 Sep 2018; P64-P66. (in Thai)

[3] Kraipakorn D., King of Chiang Mai's "Khum Luang"/"Wiang Khaew" in the era of King Chulalongkorn The untold story in Siam-Chronicle and traces founded in other sources; Available at: https://so04.tci-thaijo.org/index.php/NAJUA/article/download/10625/11328/26797. (in Thai)

[4] Promchart P. and Suwatcharapinun S., Exploring Chiang Mai architecture in political transition period between 1884-1947, Available at: https://so02.tci-thaijo.org/index.php/jed/article/view/68363. (in Thai)

[5] Meechoobot W., 'Wiang Kaew' from 'Khum Luang' to 'Kok Luang' in Nakhon Chiang Mai, Available at: www.silpa-mag.com/history/article_5445?fdclid. (in Thai)

[6] Kasetsart University team, *Geophysical exploration inside KLWKP, Sriphum subdistrict, Mueang Chiang Mai district, Chiang Mai City*, Academic Report, Kasetsart University, Thailand, 2013. (in Thai)

[7] Akarapotiwong P., Palaces in Chiang Mai Old City: A Case Study of Chao Singh Kaew's Palace, Available at: https://so04.tci-thaijo.org/index.php/NAJUA/article/download/232280/158613/784243. (in Thai)

[8] Sukkasem, Y., *Archaeological operation around Burirat's house*, Archaeological Report, The 8th Regional Fine Arts Department, 2017. (in Thai)

[9] Everett M.E., *Near Surface Geophysics*, Cambridge University Press, Cambridge, 2013.

[10] Hizem M., Budan H. and Deville B., *Society of Petroleum Engineers Technical Papers*, 2008; **116130**: 1-21. DOI 10.2118/116130-MS.

[11] Davis J.L. and Annan, A.P., *Geophysical Prospecting*, 1989; **37**: 531–551. DOI 10.1111/j.1365-2478.1989.tb02221.x.

[12] Conyers L.B., *Ground-penetrating radar and magnetometry for buried landscape analysis*, AltaMira Press, Maryland, USA, 2013.

[13] Harry M.J., *Ground penetrating radar: theory and applications*, Elsevier Science, Amsterdam, The Netherlands, 2009.

[14] Pompranee P., *Agronomy Handout*, Faculty of Science and Technology, Nakhon Pathom Rajabhat University, 2017. (in Thai)

[15] Abdulrazzaq Z.T., Thabit J.M. and Al-Khafaji A.J., *Bollettino di Geofisica Teorica ed Applicata*, 2021; **62**: 159-172. DOI 10.4430/bgta0338.

[16] Ristic A., Govedarica M., Pajewski L., Vrtunski M. and Bugarinovic Z., *Sensors*, 2020; **607**: 1-20. DOI 10.3390/s20030607.

[17] Bianco C., Giorgi L.D. and Persico R., *Remote Sensing*, 2019; **11**: 1478-1503. DOI 10.3390/rs11121478.

[18] Masini N., Leucci G, Vera D. and Lasaponara R, *Sensors*, 2020; **20**: 2870-2885. DOI 10.3390/s20102869.